Recycling of Brush Polymer Containing Iridium Photocatalyst supported on Glass Balls

Audrey Beillard, Julien a L Renault, Duc-Hahn Nguyen, Warren Lhuillier, Jean-Luc Renaud, Aurélie Vicente, Sylvain Gaillard

ARTICLE

Recycling of Brush Polymer Containing Iridium Photocatalyst supported on Glass Balls.

Received 00th January 20xx,
Accepted 00th January 20xx

DOI: 10.1039/x0xx00000x

Audrey Beillard,[a] Julien A. L. Renault,[a] Duc-Hahn Nguyen,[a] Warren Lhuillier,[a] Jean-Luc Renaud,[a] Aurélie Vicente,[b] and Sylvain Gaillard.*[a]

The synthesis of the first glass-supported iridium photocatalyst is reported. The use of brush polymer to covalently link the iridium ancillary ligand (2,2-bipyridine derivative) to the glass, allows 0.5 wt% of iridium loading on 9 – 13 µm glass balls. Cross dehydrogenative coupling (CDC) was selected as a benchmark reaction of photoredox reaction. The photocatalytic material has been recycled 10 time without loss of activity. To the best of our knowledge, this is the first functionalization of glass spheres for photocatalytic applications.

Introduction

For several decades, a huge effort had been made to develop eco-compatible processes. As a matter of fact, photoredox catalysis has gained a great interest because light can be seen as an environmentally friendly reagent. Light induced processes offer now the opportunity to develop new strategies as evidenced in literature.[1,2] Efforts have also been devoted to highly efficient reactions using Earth-abundant transition metal photocatalysts but catalyst loading is usually higher than with noble metals.[3,4] In addition, iridium complexes demonstrated to be useful tool in various photocatalytic processes including dual catalysis[5] or enantioselective synthesis.[6,7] So, the recycling of platinum metal photocatalysts or their incorporation on immobilized phase in flow chemistry process can be highly advantageous for further industrial developments. Nevertheless, heterogeneous supported photocatalysts, and their recycling remain scarce. Only few examples of supported iridium photocatalyst were described with SiO_2,[8-10] metal organic frameworks,[11-13] or polymers[14-24] as support. If transparency toward visible light is considered, those materials might present a drawback, and glass or quartz would be more suitable for further development in photoredox flow chemistry processes. The main bottleneck of glass surfaces, compare to silica and MOFs, is the low specific surface and the number of chemical functions that can be functionalized. Taking advantage of previous studies on transition metal incorporated in polymers,[25] the functionalization of glass surface to increase the number of coordination sites was envisaged to tackle this issue. In the present study, a proof of concept depicting glass spheres of 9 – 13 µm functionalized by 0.5 wt% of an iridium photocatalyst is presented. Additionally, cross dehydrogenative coupling reaction[26-31] (CDC) between tetrahydroquinoline and nitromethane, as model reaction, has been performed with this new heterogeneous photocatalytic material. Of note, this photocatalyst material has been recycled 10 times without any loss of activity.

Results and discussion

For the synthesis, the surface of the glass balls (**GS**) were firstly cleaned using piranha solution. For the chemical characterization of cleaned **GS**, ^{1}H MAS NMR was performed and silanol content was measured at 6.4 µmol per gram of glass balls (see ESI, Figure S1). Then, the Brunauer-Emmett-Teller surface area (BET) was measured and a value of 1.67 $m^2.g^{-1}$ was found, indicating an absence of porosity. The first synthetic step consisted in the silanization of **GS** by a 5 wt% of chlorosilane derivative **1** to furnish **GS-ini** (Scheme 1), i.e. **GS** incorporating atom transfer radical polymerization (ATRP) initiators. Then, poly(2-hydroxyethyl methacrylate) (**PHEMA**) brushes were grown in the presence of $CuCl/CuBr_2$/2,2-bipyridine catalytic system using 2-hydroxyethyl methacrylate **2** as monomer. At the end of the reaction, an inseparable mixture of **GS-PHEMA** and non-crafted **PHEMA** was obtained (Scheme 1).[32,33] Of note, a brief screening of the reaction conditions has shown that all component of the catalytic cocktail were essential for the polymerization process. Then, nucleophilic substitution of the hydroxy group of the crude **GS-PHEMA** was performed with non-symmetrically substituted 4,4'-bipyridine derivative **3** leading to **GS-bipy** (Scheme 1). Importantly, the non-crafted PHEMA formed in the previous step can be removed by washing

[a] Normandie University, LCMT, ENSICAEN, UNICAEN, CNRS, 6 Bd du Maréchal Juin, 14050 Caen, France.
[b] Normandie University, LCS, ENSICAEN, UNICAEN, CNRS, 6 Bd du Maréchal Juin, 14050 Caen, France.

† Electronic Supplementary Information (ESI) available: experimental details, materials characterization (NMR spectroscopy, Fluorescence spectroscopy, UV-visible spectroscopy, Electrochemistry, HRMS analysis). See DOI: 10.1039/x0xx00000x

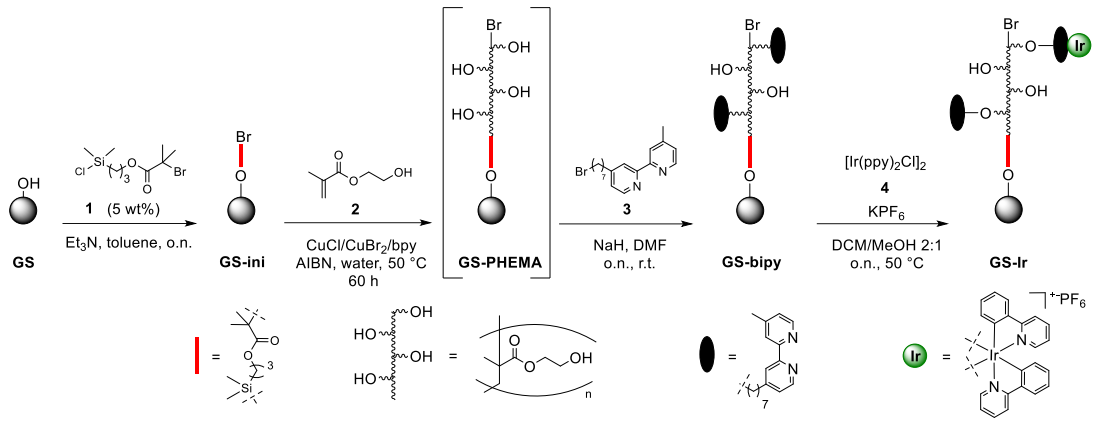

Scheme 1. Synthetic pathway for the preparation of the heterogeneous iridium-functionalized glass spheres **GS-Ir**.

the material with diethylether (see ESI). **GS-Ir$_{518}$** was finally obtained by coordination of the iridium metal centers following adapted known procedure in the presence of the iridium dimer $[Ir(ppy)_2Cl]_2$ **4**.[34]

^{1}H and ^{13}C MAS NMR were performed on each purely isolated material, i.e. **GS-ini**, **GS-bipy** and **GS-Ir$_{518}$** and indicate that all framework of the brush polymer, as well as, the ATRP initiator and ligands, were incorporated on the **GS** (Figure S2-S5). In details, signals at 8.5 and 6.9 ppm were assigned to aromatic protons of the iridium complex ligands. Signals at 2.0 and 1.4 were attributed to CH_2 and CH_3 of the polymer chain (Figure S5). In order to observe the signals of the CH_2 of the brush part, ^{1}H echo MAS NMR experiment were conducted to decrease the intensity of the labile proton of the Si-OH residual function on the glass surface (Figure S6). In these conditions, signals of the two CH_2 were detected at 4.95 and 3.8 ppm (Figure S6) and even the integration with a ratio 2:3 between the CH_2 at 2.0 ppm and the CH_3 at 1.4 ppm confirms the previous attribution. Finally, a signal at 0.1 ppm was observed in the ^{1}H MAS NMR and was assigned to the CH_3 group of the silane function of the ATRP initiator. ^{13}C MAS NMR spectroscopy was also performed on **GS-ini**, **GS-bipy** and **GS-Ir$_{518}$** and supported the ^{1}H MAS NMR analyses. In details, ^{13}C MAS NMR spectrum of **GS-ini** exhibited a signal at 0 ppm that was assigned to the methyl groups of the ATRP initiator (Figure S2). After ATRP reaction and functionalization of **GS-PHEMA** by the bipy derivative **3**, the ^{13}C MAS NMR spectrum of **GS-bipy** showed appearance of the carbon atom assigned to the CH_3 and CH_2 frameworks of the brush polymer at 11.5 and 45.0 ppm, respectively (Figure S4). Finally, the ^{13}C MAS NMR spectrum of **GS-Ir$_{518}$** confirmed the formation of the iridium complexes as an additional signal at 130 ppm was observed and was assigned to the aromatic carbon atoms of the ligands (Figure S4).

CPMAS $\{^1H\}$-^{29}Si NMR experiment was performed on **GS-Ir$_{518}$** and compared to the same analysis of **GS**. The comparison of those NMR spectra allowed to estimate that approximately 66 % of the silanol moieties were functionalized by compound **1** (Figure S7). Unfortunately, attempts to quantify the absolute quantity of reacting initiator **1** by CPMAS $\{^1H\}$-^{29}Si NMR was unsuccessful after the two steps synthesis furnishing **GS-bipy**, as CPMAS is known to be a qualitative experiment.

To confirm again the formation of **GS-Ir$_{518}$** and also to compare its photocatalytic activities with homogeneous analogs, the well-defined $[Ir(ppy)_3]$ **5**,[35] $[Ir(ppy)_2(dtbby)][Cl]$ **6**[36] and $[Ir(ppy)_2(\mathbf{3})][PF_6]$ **7**,[34] were prepared (Figure 1). Complex **7** is the analogous iridium complex present in **GS-Ir$_{518}$** and was first used as reference for photophysical characterization of **GS-Ir$_{518}$**.

The reflectance and phosphorescence spectroscopies of **GS-Ir$_{518}$** in solid state were achieved and compared to UV-visible and phosphorescence spectra of **7** in solution (Figure 2). The diffuse reflectance of **GS-Ir$_{518}$** in solid state showed maxima centered at 276, 305, 390, 420 and 472 nm. In comparison, UV-visible spectrum of complex **7** in dichloromethane solution exhibited very similar profile with maxima found at 259 (^{1}ILCT), 272 (^{1}ILCT), 309 (^{1}ILCT), 380 (^{1}LLCT), 415 (^{1}MLCT) and 472 (^{3}MLCT) nm (Figure 2).[37]

Then, **GS-Ir$_{518}$** was subjected to phosphorescence spectroscopy in solid state (Figure 2). As the emission spectrum was presenting several scatterings, the original measurement was unclear (see ESI Figure S11). After removing background and mathematical deconvolution, maximal λ_{em} was found to be centered at 515 nm (see Figure 2 for modified emission spectra and see Figure S11 to S15 in ESI for measured emission spectra and mathematical treatment). By comparison, phosphorescent emission of complex **7** in dichloromethane disclosed a maximal wavelength at 580 nm. Such blue-shifted emission of supported iridium complex on silica, compared to its analogous in solution, was already observed by Yamashita and co.[9] and attributed to a "rigidochromic" effect.[38] Nevertheless, all these analyses tend to validate the incorporation of an iridium complex into a brush polymer, and consequently the synthesis of the new supported **GS-Ir$_{518}$**.

Figure 1. Homogeneous type iridium complexes **5**-**7**.

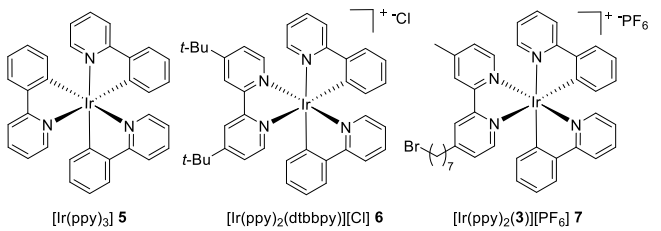

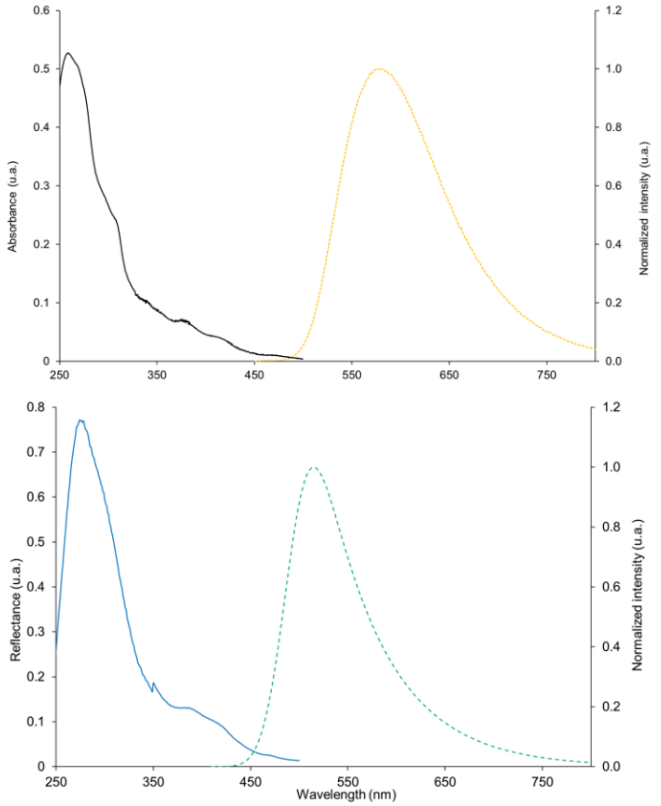

Figure 2. Top: Absorption (black curve) and normalized emission spectra (dotted yellow curve, λ_{ex} = 380 nm) of [Ir(ppy)$_2$(**4**)][PF$_6$] **7** in dichloromethane solution (C = 10^{-5} M); Bottom: Diffuse reflectance spectra (blue curve) and normalized solid emission spectra (dotted green curve, λ_{ex} = 330 nm) of **GS-Ir$_{518}$**.

After these photophysical evidences of the presence of phosphorescent iridium complex coordinated to the bipyridine functionalized brush polymer, quantification of iridium element in **GS-Ir$_{518}$** was investigated by ICP-MS and a loading of 518 ppm (0.52 wt%) in **GS-Ir$_{518}$** was measured. Thanks to the brush polymer, the iridium content of **GS-Ir$_{518}$** is comparable to those obtained with silica-functionalized metal complexes albeit the specific surface of glass is lower than the one of silica.[9,39,40]

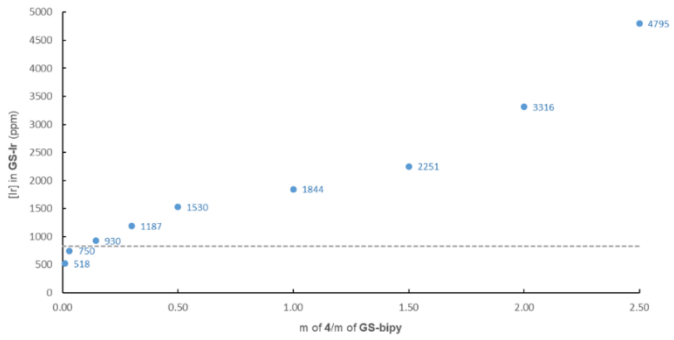

Figure 3. Iridium concentration [Ir] depending on the initial mass ratio of iridium dimer **4** and **GS-bipy** for the synthesis of **GS-Ir**. Dash line represents the potential concentration of [Ir] if all silanol on **GS** surface where mono-functionalized by a bipy ligand.

Table 1. Iridium concentration [Ir] reached in **GS-Ir** with different **4**/**GS-bipy** ratio during the coordination step.

Entry	**4**/**GS-bipy** ratio[a]	[Ir] (ppm)[b]
1	0.01	518
2	0.03	750
3	0.15	930
4	0.30	1187
5	0.50	1530
6	1.00	1844
7	1.50	2251
8	2.00	3316
9	2.50	4795

[a] Mass ratio of iridium dimer 4 and GS-bipy. [b] Determined by ICP-MS.

Further investigations were undertaken to explore the possibility to vary the iridium concentration [Ir] in the **GS-Ir** material, by changing the mass ratio between iridium dimer **4** and **GS-bipy** from 0.01 to 2.50 during the coordination step. All resulting new **GS-Ir** were then subjected to ICP-MS analysis to quantify the concentration of the iridium complexes [Ir]. Results are summarized in **Table 1** and shown in **Figure 3**.

Additionally, ^{1}H MAS NMR allowed us to estimate that a maximum iridium concentration [Ir] of 825 ppm could be reached if all silanol frameworks were mono-functionalized by one bipy ligand. Introducing **GS-bipy** materials with different mass ratio of **4**/**GS-bipy** from 0.01 to 2.5, [Ir] increased gradually from 518 to 4795 ppm, respectively. Thanks to the brush polymer, an increase of almost 6 time of the [Ir] can be achieved compare to an unfunctionalized **GS** if the surface were solely mono-functionalized by a bipy ligand.

With this characterized new **GS-Ir** material in hands, the next step in this study was its evaluation in photoredox reaction, and more specifically in CDC reaction using 2-phenyltetrahydroisoquinoline **8** in nitromethane solution, as a model reaction.[26-31] Due to the low iridium loading in **GS-Ir$_{518}$**, the evaluation was initiated with a mass of **GS-Ir$_{518}$** corresponding to a PC concentration of 0.1 mol%. Results are summarized in table 2.

Table 2. Photocatalytic evaluation of **GS-Ir$_{518}$** vs. complexes **5**-**7** in CDC reaction.

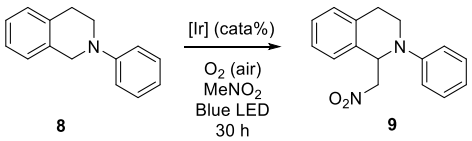

8 **9**

Entry	Catalyst (x mol%)	Yield (%)[a]
1	**GS-Ir$_{518}$** (0.1)[b]	71
2	**GS-Ir$_{518}$** (0.1)	81
3	**5** (0.1)	27
4	**5** (1)	81
5	**6** (1)	44
6	**7** (1)	62
7	-[c]	24

[a] Yield were determined by ^{1}H NMR analysis. [b] Reaction time 24 h. [c] without any PC.

Gratifyingly, alkylated compound **9** was obtained in 71% ^{1}H NMR yield after 24 h under blue light irradiation (455 nm, 38 W) (Table 2, entry 1). Increasing the reaction time, from 24 to 30 h, improved the ^{1}H NMR yield from 71 to 81% (Table 1, entries 1-2). For comparison, complex [Ir(ppy)$_3$] **5** was engaged in this CDC reaction with a catalyst loading of 0.1 mol%, and 27 % of yield were reached. Of note, a loading of 1 mol% was required to attain the same result than the one with 0.1 mol% of **GS-Ir$_{518}$** (Table 2, entry 4 vs. entry 2).[4] Additionally, in the presence of 1 mol % of complex **6** or **7**, homogeneous analog of **GS-Ir$_{518}$**, only 44 and 62 % of alkylated compound were obtained, respectively (Entries 5 and 6). Finally, in the absence of iridium complex, 24 % ^{1}H NMR yield were observed. This result correlates data found in the literature.[41]

Comparison of the reaction kinetics in the presence of the new materials **GS-Ir** (having various iridium complexes concentration), the complex [Ir(ppy)$_3$] and also in the absence of any PS was conducted over an 8 h period under blue light irradiation. Figure 4 shows that all supported iridium photocatalyst materials **GS-Ir** provided higher conversions of compound **8** than reaction using [Ir(ppy)$_3$] or in absence of iridium photocatalyst after 1 h under irradiation, 28 to 72 % for **GS-Ir** vs 17 % when using [Ir(ppy)$_3$] (Figure 4). After 8 h under irradiation, [Ir(ppy)$_3$] achieved 69 % conversion of compound **8** whereas **GS-Ir** reached conversion between 76 to 88 % for the same time (Figure 4).

Analyses of the ^{1}H NMR spectra of the various reaction crudes (see ESI, figure S17) at the end of the photocatalysis showed the formation of the expected CDC compound **9** and, in some case, an unreported by-product **10** identified as a nitrile derivative[42] and an already observed by-product identified as the lactam **11** (Scheme 2).[43]

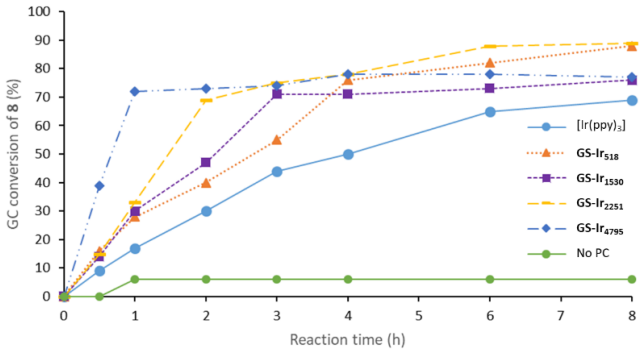

Figure 4. Conversion of compound **8** using **GS-Ir** materials, [Ir(ppy)$_3$] or in absence of PC.

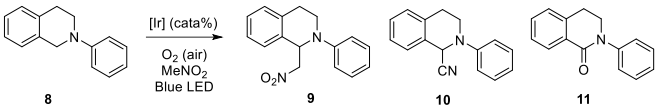

Scheme 2. Photocatalyzed-CDC reaction from compound **8** leading to compounds **9**-**11**.

To have a better understanding of all these processes, electrochemical analysis and kinetics were undertaken. Cyclic voltammetry was initially performed on **GS-Ir(III)** material but did not furnish satisfying results. In order to estimate the redox potentials of **GS-Ir(III)*** at excited state, we turned our attention to complex **7**, the homogeneous congener of **GS-Ir(III)**. Cyclic voltammetry of **7** indicated that the redox potentials for the couple [Ir(IV)]/[Ir(III)] and [Ir(III)]/[Ir(II)] were 1.17 and -1.52 V vs. SCE, respectively (see ESI Figure S18 and Table S1). Then, considering the emission wavelength at 580 nm for complex **7**, the redox potentials in the excited state for **7** were respectively approximated at - 0.97 V vs SCE for [Ir(IV)]/[Ir(III)]* and 0.62 V vs SCE for [Ir(III)]*/[Ir(II)] (approximation achieved with E^{00} = 2.14 V).[37] We hypothesized that the redox potentials of complex **7** could be similar to those of our new photoactive materials **GS-Ir(III)** and consequently these values were used for further study and to the proposed mechanisms (Figure 5-7). The formation of compounds **9**-**11** was explained based on three consecutive distinct catalytic cycles. Figure 5 depicts the formation of compound **9** which is the first product formed during our photocatalytic conditions and is similar to the mechanism usually reported in literature.

In details, **GS-Ir(III)** could be excited under blue light irradiation into **GS-Ir(III)***. Then, all the photocatalytic sequence could be initiated via an oxidative quenching. Indeed, the most favorable single electron transfer (SET) could generate the reduction of O_2 into its oxygen radical anion $O_2^{\cdot-}$ ($E(O_2/O_2^{\cdot-})$ = - 0.75 V vs SCE)[44] with concomitant oxidation of **GS-Ir(III)*** into **GS-Ir(IV)** ($E([Ir(IV)]/[Ir(III)]^*)$ = - 0.97 V vs SCE, see ESI Table S1). Then, regeneration of the photocatalyst **GS-Ir(III)** could occur through another SET between **8** and **GS-Ir(IV)** ($E([Ir(IV)]/[Ir(III)]$ 1.17 V vs SCE) leading to the radical cation **8**$^{\cdot+}$ ($E(\mathbf{8}/\mathbf{8}^{\cdot+})$ = 0.83 V vs SCE).[44] Then, reaction of $O_2^{\cdot-}$ with the radical cation **8**$^{\cdot+}$ led to the iminium **8**$^+$ with hydroperoxide anion HO_2^- as counterion. Finally, the reaction of nitromethane with the iminium **8**$^+$ furnished the expected compound **9** and H_2O_2.[44] As consequence of this first photocatalytic process, H_2O_2 could accumulate in time and might be responsible of the evolution of compound **9** into firstly compound **10** which is reported, to the best of our knowledge for the first time in a CDC reaction.

ARTICLE

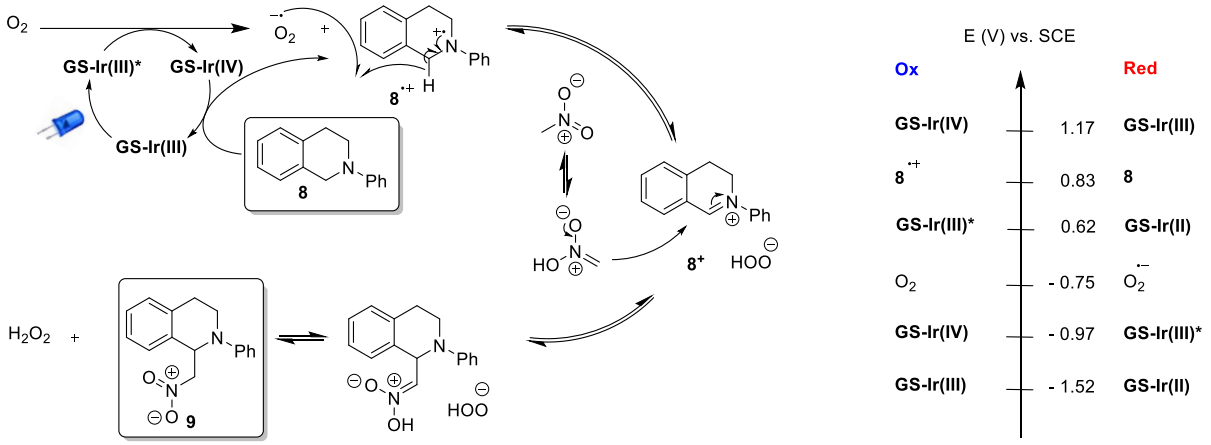

Figure 5. Proposed mechanism for the formation of **9**.

Figure 6 describes a possible pathway to explain the formation of **10** from **9** involving H_2O_2, as protons and electrons source, and the immobilized iridium complex **GS-Ir(III)**, and regeneration of O_2. The latter supports and explains the CDC reaction between nitromethane and compound **9** in closed vessel.

As shown in figure 6, H_2O_2 (E_{ox} = 0.44 V vs SCE)[45] could serve as a reductant to allow the transformation of two equivalent of Ir(III)]* to [Ir(II)] ($E_{[Ir(III)]*/[Ir(II)]}$ = 0.62 V vs SCE). This reduction would produce then dioxygen involved in oxidation steps (see vide supra - Figure 5 and vide infra - Figure 7) and protons able to react with compound **9**. Protonation of **9** followed by tautomerization and dehydration step might lead to an hydroxynitrilium intermediate. Such intermediate from a nitro derivative was previously described in literature for the Nef and Meyer reaction[46] and could lead to the formation of the nitrile oxide **12**. As the oxidation process of H_2O_2 into O_2 is a 2 electrons redox process, two GS-Ir(III)* would accept one electron and be reduced into two GS-Ir(II) species. Then, these two GS-Ir(II) species could be oxidized by two SET with **12** in acidic conditions.[47] This process could give the nitrile compound **10** and is consistent with the electrosynthesis of nitrile from oxime via cathodic reduction of nitrile oxide.[48] Indeed, the lead cathode used in this study has a reducing potential E(Pb^{2+}/Pb) of around -0.47 V,[49] and Ir(II)/Ir(III) redox couple of **GS-Ir** appears to have a higher reduction power (-1.52 V vs SCE) and should be able to perform this redox step.

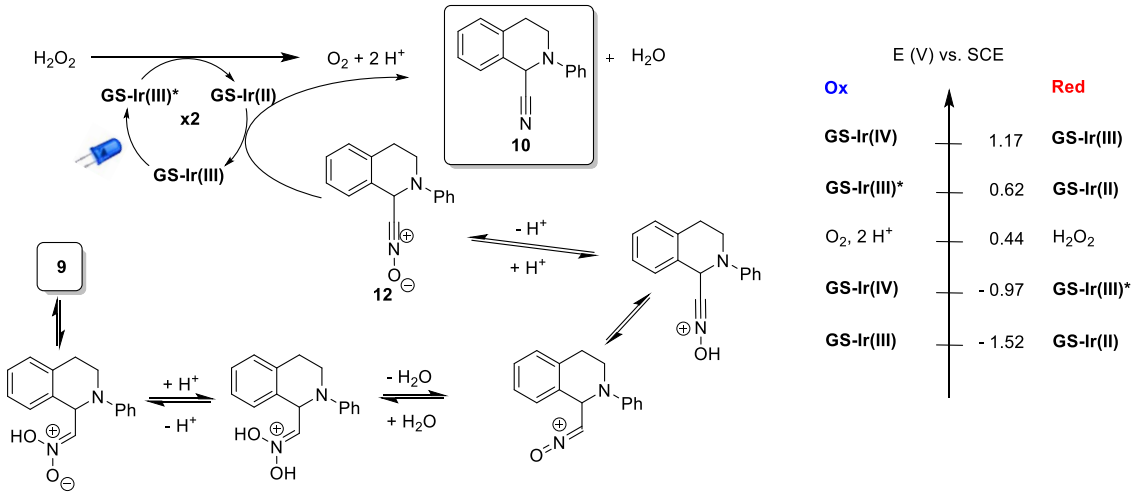

Figure 6. Proposed mechanism for the formation of **10**.

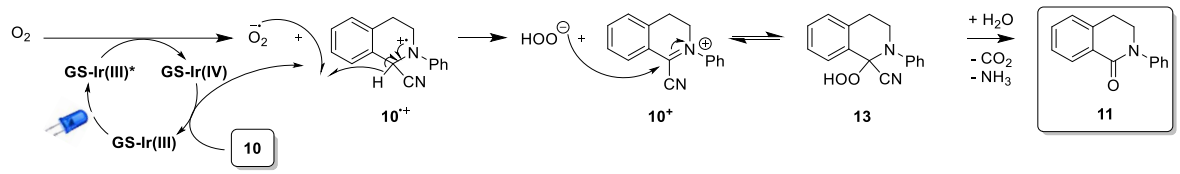

Figure 7. Proposed mechanism for the formation of **11**.

This pathway could also be consistent with the fact that the formation of **10** occurred with a higher rate when the concentration of iridium complexes [Ir] increased on the **GS-Ir(III)** material (vide supra). We assume that the functionalized brush-polymer **GS-Ir(III)** brings the iridium PS species close to each other, allowing a more efficient two electrons/two protons transfer for the formation of **10**.

Finally, figure 7 shows the proposed mechanism for the photocatalytic Reissert compound oxidation furnishing the lactame **11**.[50,51] This synthesis might be initiated via the traditional oxidative cycle allowing the formation of $O_2^{\cdot-}$ and the radical cation $\mathbf{10}^{\cdot+}$, similar to the formation of $\mathbf{8}^{\cdot+}$. Hydride abstraction furnished the iminium intermediate $\mathbf{10}^{+}$. A subsequent addition of HOO^- to the latter could generate the peroxo-nitrile intermediate **13**. Then, in the presence of in situ generated water, the lactame **11** would be obtained after the loss of CO_2 and NH_3.[50,51]

Formation of both compounds **10** and **11** over time was investigated by performing kinetics of the photocatalytic reaction (Figure 8). Interestingly, 88 % conversion of **8** into **9** was observed after 6 h using **GS-Ir$_{518}$**. Then, the first 5 % of a mixture of **10** and **11** was observed after 8 h of photocatalysis and their formation slightly increased until 11 % after 30 h of reaction.

In addition to the kinetic study for **GS-Ir$_{518}$**, the same experiment was conducted with **GS-Ir$_{2251}$** and **GS-Ir$_{4795}$**. Figure 9 shows the kinetic profiles of both CDC reaction with compound **8**.

Importantly, the reaction time to reach 75 % of conversion was shortened compared to **GS-Ir$_{518}$** (around 1.5 h and 1 h for **GS-Ir$_{2251}$** and **GS-Ir$_{4795}$**, respectively). Not surprisingly, increasing the catalyst loading accelerated the kinetic of the CDC reaction. Likewise, the formation of the mixture of **10** and **11** was observed in all photocatalytic reactions. Higher the concentration of iridium complexes [Ir] in **GS-Ir** material, faster the formation of **10** and **11** was detected. Of note, compounds **10** and **11** became the major products after 30 h of photocatalytic reaction with **GS-Ir$_{2251}$** or **GS-Ir$_{4795}$**.

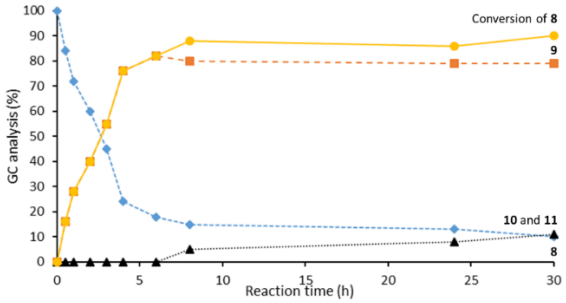

Figure 8. Kinetic of the CDC reaction photocatalyzed by **GS-Ir$_{518}$**.

As the amount of **10** and **11** remains below 10% after 24 h in the presence of **GS-Ir$_{518}$**, we use this immobilized photocatalyst to evaluate the recycling in the model CDC reaction. Experimentally, a simple centrifugation followed by removal of the supernatant solution containing the organic compounds furnished the crude immobilized **GS-Ir**, which was reengaged directly with fresh starting materials. No loss of photocatalytic activity was noticed (69 % ±2%) except for the 6th run (54 %) attributed to an irradiation or stirring issue, as initial yield was recovered at the 7th run and until the 10th run. Of note, the cumulative TON on 10 runs reached 6760 (Figure 10). Additionally, these studies shown an efficient photoactivity for at least 240 h under irradiation for **GS-Ir$_{518}$**.

After the last recycling run, ICP-MS analysis was performed both on **GS-Ir$_{518}$** material and also on the crude mixture. No iridium was detected in the crude solution but a loading of 233 ppm was determined and found in the recovered **GS-Ir$_{518}$**. As no decrease of catalyst activity of **GS-Ir** was observed after 10 runs of 24 h and no iridium leaching was detected in the reaction mixture, the drop of iridium complex concentration was attributed to a solvent or reagent trap within the solid as reported before for polymer-supported photocatalysts.[52–54]

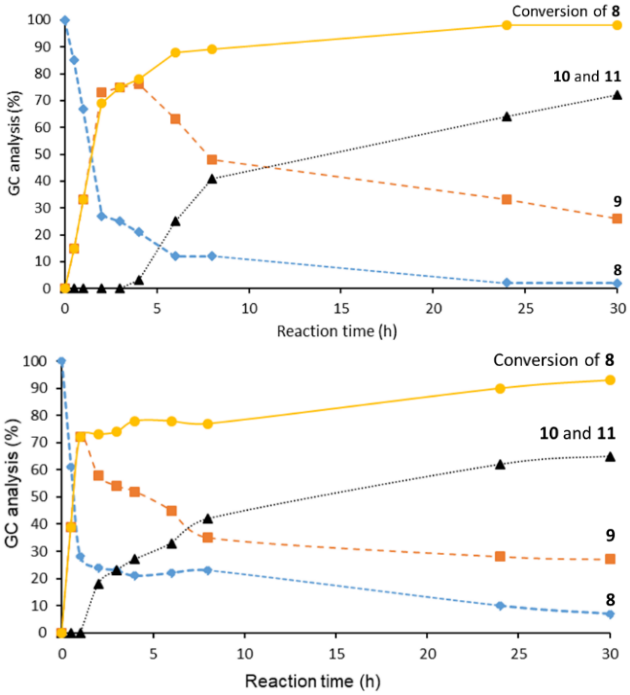

Figure 9. Kinetics of the CDC reaction photocatalyzed by **GS-Ir$_{2251}$** (above) and **GS-Ir$_{4795}$** (below).

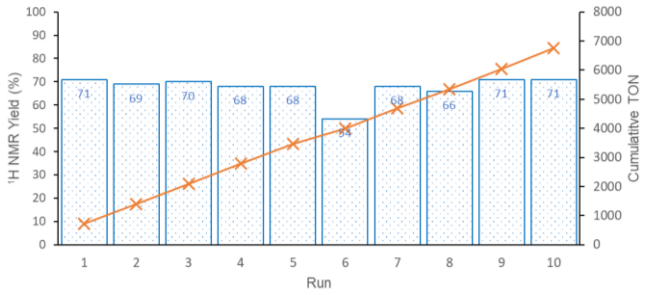

Figure 10. Recycling of **GS-Ir** and cumulative TON over the 10 recycling runs.

Conclusions

This study reports the proof of concept of a glass sphere surface functionalization by brush polymer coordinated-iridium photocatalyst. Characterization has been achieved by reflectance and phosphorescent spectroscopy. Dosage of the iridium loading by ICP-MS revealed that this new photocatalytic material contained as much photocatalyst as most of the silica-based materials reported in the literature, even if glass is known to possess a lower specific surface. The CDC reaction photocatalyzed by **GS-Ir** exhibited better activity than their analogous iridium complexes in homogeneous conditions. Moreover, these catalysts can be recycled, at least, 10 times without any loss of activity, reaching a cumulative TON of 6760. To conclude, this new architecture of supported photocatalytic system may pave the way to further development in stationary phase for flow chemistry process. Development on glass spheres of bigger sizes as well as incorporation of this material in flow photochemistry process in an ongoing research in our laboratories.

Author Contributions

The manuscript was written through contributions of all authors. All authors have given approval to the final version of the manuscript.

Conflicts of interest

There are no conflicts to declare.

Acknowledgements

This work was supported by the "Ministère de la Recherche et des Nouvelles Technologies", CNRS (Centre National de la Recherche Scientifique) for the EMERGENCE@INC2018 grant (D-HN) and the LABEX SynOrg (ANR-11-LABX-0029). S. G. acknowledges the “Région Normandie” (A.B.) for their fundings and the ANR for the grant for the project VECTRIUM (ANR-19-CE18-0011-02).

Notes and references

1 A. Dandia, P. Saini, R. Sharma and V. Parewa, *Green Sustainable Process for Chemical and Environmental Engineering and Science*; Inamuddin, Boddula, R., Asiri, A. M., Eds.; Elsevier, 2020; pp 155.
2 N. Hoffmann, *Chem. Rev.*, 2008, **108**, 1052.
3 C. K. Prier, D. A. Rankic and D. W. C. MacMillan, *Chem. Rev.*, 2013, **113**, 5322.
4 K. Teegardin, J. I. Day, J. Chan and J. Weaver, *Org. Process Res. Dev.*, 2016, **20**, 1156.
5 K. L. Skubi, T. R. Blum and T. P. Yoon, *Chem. Rev.*, 2016, **116**, 10035.
6 H. Huo, X. Shen, C. Wang, L. Zhang, P. Röse, L.-A. Chen, K. Harms, M. Marsch, G. Hilt and E. Meggers, *Nature*, 2014, **515**, 100.
7 L. Zhang and E.Meggers, *Acc Chem Res*, 2017, **50**, 320.
8 Z. Hao, S. Li, J. Sun, S. Li and F. Zhang, *Applied Catalysis B: Environmental*, 2018, **237**, 366.
9 K. Mori, M. Tottori, K. Watanabe, M. Che and H. Yamashita, *J. Phys. Chem. C*, 2011, **115**, 21358.
10 S. M. Soria-Castro, B. Lebeau, M. Cormier, S. Neunlist, T. J. Daou and J.-P.Goddard, *Eur. J. Org. Chem.*, 2020, **2020**, 1572.
11 L.-Q. Wei and B.-H. Ye, *ACS Appl. Mater. Interfaces*, 2019, **11**, 41448.
12 L. Qiu, A. Dong, S. Zhang, S. Wang, Z.Chang, Y.Lu, Z. Sui, L. Feng and Q. Chen, *J Mater Sci*, 2020, **55**, 9364.
13 C. Wang, Z. Xie, K. E. de Krafft and W.Lin, *J. Am. Chem. Soc.*, 2011, **133**, 13445.
14 H.-P. Liang, Q. Chen and B.-H. Han, *ACS Catal.*, 2018, **8**, 5313.
15 F. Peng, P. Zhi, H. Ji, H. Zhao, F.-Y. Kong, X.-Z.Liang and Y.-M. Shen, *RSC Adv.*, 2017, **7**, 19948.
16 P. Zhi, Z.-W. Xi, D.-Y. Wang, W. Wang, X.-Z. Liang, F.-F. Tao, R.-P. Shen and Y.-M. Shen, *New J. Chem.*, 2019, **43**, 709.
17 J. Ma, F. Strieth-Kalthoff, T. Dalton, M. Freitag, J. L. Schwarz, K. Bergander, C. Daniliuc and F Glorius, *Chem*, 2019, **5**, 2854.
18 W.-J. Yoo and S. Kobayashi, *Green Chem.*, 2014, **16,** 2438.
19 X. Zhang, Y. Li, X. Hao, K. Jin, R. Zhang and C Duan, *Tetrahedron* 2018, **74**, 7358.
20 D. Rackl, P. Kreitmeier and O. Reiser, *Green Chem.*, 2016, **18**, 214.
21 Z. Xie, C. Wang, K. E. deKrafft and W. Lin, *J. Am. Chem. Soc.* 2011, **133**, 2056.
22 C. Wang, Z. Xie, K. E. deKrafft and W. Lin, *ACS Appl. Mater. Interfaces*, 2012, **4**, 2288.
23 L. Pan, M.-Y. Xu, L.-J. Feng, Q. Chen, Y.-J. He and B.-H Han, *Polym. Chem.*, 2016, **7**, 2299.
24 Y. Pan, N. Zhang, C.-H. Liu, S. Fan, S. Guo, Z.-M. Zhang and Y.-Y. Zhu, *ACS Catal.*, 2020, **10**, 11758.
25 A. E. Fernandes, A. Dirani, C. d’Haese, G. Deumer, W. Guo, P. Hensenne, F. Nahra, X. Laloyaux, V. Haufroid, B. Nysten, O. Riant and A. M. Jonas, *Chemistry – A European Journal*, 2012, **18**, 16226.
26 F. A. Luzzio, *Tetrahedron*, 2001, **57**, 915.
27 L. Dong and F.-E. Chen, *RSC Adv.*, 2020, **10**, 2313.
28 S. Nidhi and P.J aya, *Mini-Reviews in Organic Chemistry* 2020, **17**, 297.

29 E. Sauvageot, R. Marion, F. Sguerra, A. Grimault, R. Daniellou, M. Hamel, S. Gaillard and J.-L. Renaud, *Org. Chem. Front.*, **2014**, *1*, 639.
30 H. Bartling, A. Eisenhofer, B. König and R. M. Gschwind, *J. Am. Chem. Soc.*, 2016, **138**, 11860.
31 A. G. Condie, J. C. González-Gómez and C. R. J. Stephenson, *J. Am. Chem. Soc.*, 2010, **132**, 1464.
32 K. L. Robinson, M. A. Khan, M. V. de Paz Báñez, X. S. Wang and S. P. Armes, *Macromolecules*, 2001, **34**, 3155.
33 S. Tugulu, A. Arnold, I. Sielaff, K. Johnsson and H.-A. Klok, *Biomacromolecules*, 2005, **6**, 1602.
34 Y. Ohsawa, S. Sprouse, K. A. King, M. K. DeArmond, K. W. Hanck and R. J. Watts, *J. Phys. Chem.*, 1987, **91**, 1047.
35 A. B. Tamayo, B. D.Alleyne, P. I. Djurovich, S. Lamansky, I. Tsyba, N. N. Ho, R. Bau and M. E. Thompson, *J. Am. Chem. Soc.* 2003, **125**, 7377.
36 J. D. Slinker, A. A. Gorodetsky, M. S. Lowry, J. Wang, S. Parker, R. Rohl, S. Bernhard and G. G. Malliaras *J. Am. Chem. Soc.*, 2004, **126**, 2763.
37 R. Bevernaegie, S. A. M. Wehlin, B. Elias and L. Troian-Gautier, *ChemPhotoChem*, 2021, **5**, 217.
38 J. McKiernan, J. C. Pouxviel, B. Dunn and J. I. Zink, *J. Phys. Chem.*, 1989, **93**, 2129.
39 K. Feng, R.-Y. Zhang, L.-Z. Wu, B. Tu, M.-L. Peng, L.-P. Zhang, D. Zhao and C.-H. Tung, *J. Am. Chem. Soc.*, 2006, **128**, 14685.
40 K. Mori, M. Kawashima, M. Che and H. Yamashita, *Angew. Chem. Int. Ed.*, 2010, **49**, 8598.
41 J. Liu, K. Zhang, Z. Chen, Z.-W. Wei and L. Zhang, *Chem. - Asian J.* 2020, **15**, 1118.
42 J. Dhineshkumar, M. Lamani, K. Alagiri and K. R. Prabhu, *Org. Lett.* 2013, **15**, 1092.
43 F. Rusch, L.-N. Unkel, D. Alpers, F. Hoffmann and M. Brasholtz, *Chem. Eur. J.*, 2015, **21**, 8335.
44 H. Bartling, A. Eisenhoefer, B. König and R. M. Gschwind, *J. Am. Chem. Soc.*, 2016, **138**, 11860.
45 W. H. Koppenol, D. M. Stanbury and P. L. Bounds, *Free radical Biology & Medecine*, 2010, **49**, 317.
46 A. Y. Sukhorukov, *Molecules*, 2023, **28**, 686.
47 K. Lammertsma and B. V. Prasad, *J. Am. Chem. Soc.*, 1993, **115**, 2348.
48 M. F. Hartmer and S. R. Waldvogel, *Chem. Commun.*, 2015, **51**, 16346.
49 A. Hazza, D. Pletcher and R. Wills, *J. Power Sources*, 2005, **149**, 103.
50 M. D. Rozwadowska and D. Brózda, *Tetrahedron Lett.*, 1978, **19**, 589.
51 M. D. Rozwadowska and D. Brózda, *Can. J. Chem.*, 1980, **58**, 1239.
52 C.-A. Wang, Y.-W. Li, X.-L. Cheng, J.-P. Zhang and Y.-F.Han, *RSC Adv.*, 2016, **7**, 408.
53 C.-A. Wang, Y.-F. Han, K. Nie and Y.-W. Li, *Mater. Chem. Front.*, 2019, **3**, 1909.
54 C.-A. Wang, J.-P. Zhang, K. Nie, Y.-W. Li, Q. Li, G.-Z. Jiao, J.-G. Chang and Y.-F. Han, *Catal. Sci. Technol.* 2021, **11**, 3799.

